Electronic Supplementary Information for

Unlocking Photovoltaic Potential: Leveraging Unique Diazo Multimembered Ring Acceptors

Mingpeng Li,‡[ab] Waqar Ali Memon,‡[a] Shilong Xiong,‡[a] Yafei Ding,[a] Yunpeng Wang,[a] Heng Li,[a] Jingwen Si,[b] Leilei Tian,*[b] Feng He*[a,c,d]

[a] Grubbs Institute and Department of Chemistry, Southern University of Science and Technology, Shenzhen 518055, China.

[b] Department of Materials Science and Engineering, Southern University of Science and Technology, Shenzhen, Guangdong 518055, China.

[c] Guangdong Provincial Key Laboratory of Catalysis, Southern University of Science and Technology, Shenzhen 518055, China.

[d] Institute of Innovative Materials, Southern University of Science and Technology, Shenzhen 518055

‡ The authors contributed equally to this work.

† Electronic supplementary information (ESI) available. See DOI: 10.1039/d4ee02841d.

* Corresponding authors: tianll@sustech.edu.cn (Leilei Tian); hef@sustech.edu.cn (Feng He)

Content

1. **Materials and synthesis…….3**
2. **Measurements and Characterizations…….8**
3. **DFT calculation…….10**
4. **Fabrication and characterization of OSCs…….10**
5. **Supplementary Figures……11**
6. **Supplementary Tables…….....26**
7. **Reference……...30**

1. Materials and synthesis

Polymer donor PM6 and the precursor BTP-HD were purchased from Solarmer Energy Inc. Other chemical reagents and solvents were purchased from commercial suppliers and used without further purification. All reactions were performed under a nitrogen atmosphere.

Synthesis of the central units 6/7/8C-2F

Scheme S1 shows the synthetic routes of 6C-2F, 7C-2F and 8C-2F. The detailed synthesis processes of the central units and the target molecules are described in the following. Figure S1-9 were the characters based on ^{1}H NMR and MALDI-TOF.

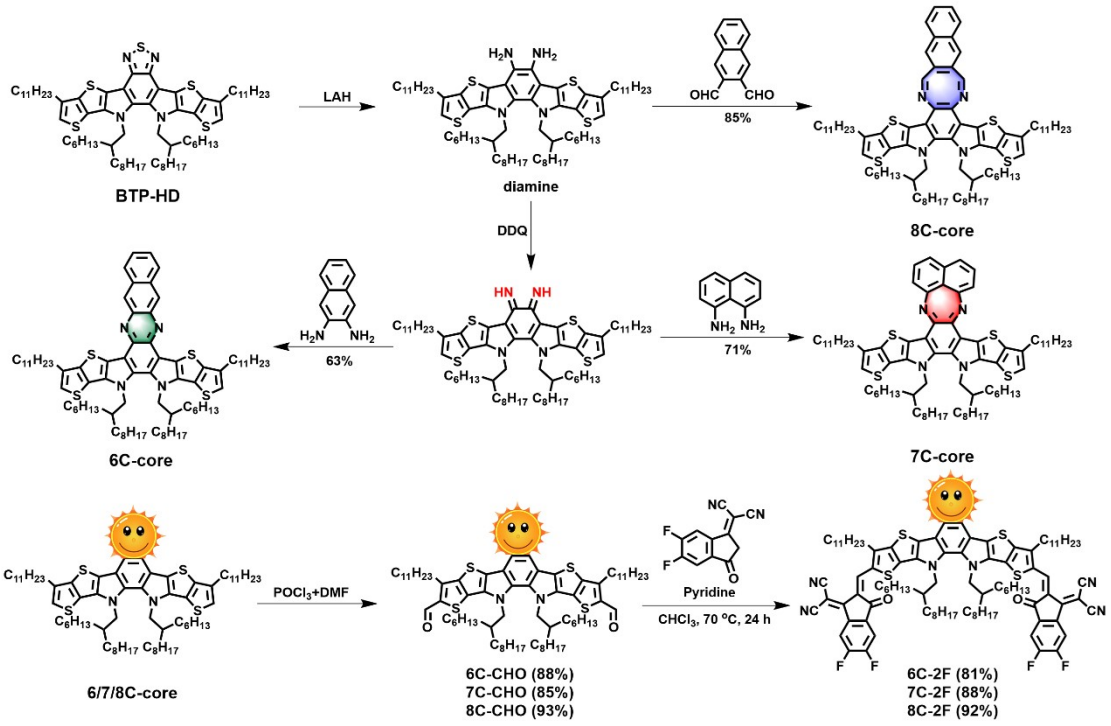

Scheme S1. Synthetic routes of 6C-2F, 7C-2F and 8C-2F.

Compound 6C-CHO[1]

To a 100 mL flask, compound BTP-HD (200 mg, 0.167 mmol) and tetrahydrofuran (THF, 20 mL) were mixed under room temperature. Then powdery lithium aluminum hydride (127 mg, 20 eq.) was added to the mixture and the reactant was stirred at 80 ℃ overnight. After this, the mixture was poured into icy dilute hydrochloric acid solution and extracted three times with ethyl acetate (EA). The organic layer was washed with

brine and dried over anhydrous Na_2SO_4. After the solvent was evaporated, a blown oily liquid (diamine) was obtained. Without further purification, the crude product was dissolved in chloroform ($CHCl_3$, 20 mL), then 2,3-dichloro-5,6-dicyano-1,4-benzoquinone (DDQ, 34 mg, 0.15 mmol, 0.9 eq.) and 2,3-diaminonaphthalene (41 mg, 0.26 mmol, 1.5 eq.) were added to the solution in turn. The reaction was stirred at RT for 24 h, and the solvent was removed under vacuum. Finally, the residue was purified by column chromatography to give compound 6C-core as a green solid (136 mg, 63%). Under the protection of argon, phosphorus oxychloride ($POCl_3$, 0.2 mL) was added to a solution of compound 6C-core (136 mg, 0.105 mmol) and N, N-dimethylformamide (DMF, 0.4 mL) in 1,2-dichloroethane (DCE, 20 mL). The reaction mixture was stirred and heated to reflux overnight and then cooled to RT. The resulting mixture was slowly quenched by the saturated solution of sodium acetate (40 mL). After being stirred at RT for 2 h. The mixture was extracted with DCM three times and the organic layer was dried over anhydrous Na_2SO_4. Finally, the target product was purified by column chromatography on silica gel with PE/DCM (v/v = 2:1) as eluent to afford compound 6C-CHO as a green solid (124 mg, 88%). ^{1}H NMR (400 MHz, $CDCl_3$) δ 10.16 (s, 2H), 9.05 (s, 2H), 8.22 (dd, J = 6.5, 3.3 Hz, 2H), 7.59 (dd, J = 6.5, 3.1 Hz, 2H), 4.67 (d, J = 7.9 Hz, 4H), 3.25 (t, J = 7.7 Hz, 4H), 2.14 (m, 2H), 1.98 (m, 4H), 1.53 (m, 4H), 1.48–1.38 (m, 6H), 1.37 – 0.76 (m, 76H), 0.76 (t, J = 7.2 Hz, 6H), 0.66 (t, J = 6.9 Hz, 6H). MS (MALDI-TOF) m/z: $[M + H]^+$ calculated for $C_{84}H_{120}N_4O_2S_4$, 1346.1500, found: 1346.1496.

Compound 6C-2F

Under the protection of argon, pyridine (0.2 mL) was added to the solution of compound 6C-CHO (65 mg, 0.048 mmol, 1.0 eq.) and 2-(5,6-difluoro-3-oxo-2,3-dihydro-1H-inden-1-ylidene) malononitrile (45 mg, 0.19 mmol, 4.0 eq.) in $CHCl_3$ (30 mL). The resulting mixture was stirred and heated to reflux for 12 h. After being cooled to RT, the solvent was removed under vacuum. The crude product was then purified by column chromatography on silica gel with PE/$CHCl_3$ (v/v = 1:1.5) as eluent to afford 6C-2F as a green solid (75 mg, 81 %). ^{1}H NMR (400 MHz, $CDCl_3$) δ 9.12 (s, 2H), 8.99

(s, 2H), 8.53 (dd, *J* = 9.9, 6.4 Hz, 2H), 8.18 (d, *J* = 7.1 Hz, 2H), 7.69 (t, *J* = 7.5 Hz, 2H), 7.63 – 7.55 (m, 2H), 4.81 (d, *J* = 7.8 Hz, 4H), 3.23 (s, 4H), 2.25 (s, 2H), 1.89 (d, *J* = 8.8 Hz, 4H), 1.40 (s, 4H), 1.35 – 1.20 (m, 34H), 1.14 – 0.96 (m, 37H), 0.85 (t, *J* = 6.5 Hz, 7H), 0.73 (t, *J* = 7.1 Hz, 7H), 0.68 (t, *J* = 6.5 Hz, 6H). ^{13}C NMR (101 MHz, CDCl3) δ 186.23, 158.34, 154.02, 146.68, 139.71, 138.64, 137.74, 136.22, 134.95, 134.23, 133.67, 133.32, 132.34, 128.36, 127.35, 126.63, 119.47, 119.39, 114.96, 114.63, 112.36, 68.00, 56.00, 39.71, 32.05, 32.03, 31.86, 31.56, 30.78, 30.14, 30.01, 29.87, 29.81, 29.78, 29.71, 29.64, 29.50, 29.41, 27.07, 26.03, 25.99, 22.81, 22.75, 22.71, 14.22, 14.20, 14.18. MS (MALDI-TOF) *m/z*: $[M + H]^+$ calculated for $C_{108}H_{125}F_4N_8O_2S_4$, 1770.8773, found: 1770.9961.

Compound 7C-CHO

To a 100 mL flask, compound BTP-HD (200 mg, 0.167 mmol) and THF (20ml) were mixed under RT. Then powdery lithium aluminum hydride (127 mg, 20 eq.) was added to the mixture and the reactant was stirred at 80 ℃ overnight. After this, the mixture was poured into icy dilute hydrochloric acid solution and extracted three times with EA. The organic layer was washed with brine and dried over anhydrous Na_2SO_4. After the solvent was evaporated, the intermediate diamine was obtained without further purification. The crude product was dissolved in $CHCl_3$ (20 mL), then DDQ (34 mg, 0.15 mmol, 0.9 eq.) and 1,8-diaminonaphthalene (80 mg, 0.26 mmol, 3.0 eq.) were added in turn. The reaction was stirred at RT for 72 h, and the solvent was removed under vacuum. Finally, the residue was purified by column chromatography to give compound 7C-core as a red solid. (153 mg, 71%) The same method was adopted to synthesize 7C-CHO. The crude product was purified by column chromatography on silica gel with PE/EA (v/v = 20:1) as eluent to afford 7C-CHO as a red solid (138 mg, 85%).^{1}H NMR (400 MHz, $CDCl_3$) *δ* 10.19 (s, 2H), 10.17 (s, 2H), 9.39 (s, 1H), 9.31 (d, *J* = 7.2 Hz, 1H), 8.26 (d, *J* = 9.2 Hz, 1H), 8.11 (d, *J* = 9.2 Hz, 1H), 7.92 – 7.71 (m, 2H), 4.74 (t, *J* = 8.8 Hz, 4H), 3.27 (q, *J* = 14.8, 7.2 Hz, 4H), 2.13 (m, 2H), 1.98 (dq, *J* = 14.8, 8.8, 7.2 Hz, 4H), 1.52 (m, 4H), 1.42 – 1.38 (m, 4H), 1.36 – 0.81 (m, 74H), 0.76 – 0.72 (t, 7.2 Hz, 8H), 0.68 – 0.62 (t, 7.2 Hz, 6H). MS (MALDI-TOF) m/z: $[M + H]^+$ calculated

for $C_{84}H_{120}N_4O_2S_4$, 1346.1500, found: 1346.1460.

Compound 7C-2F

Under the protection of argon, dry pyridine (0.2 mL) was added to a solution of compound 7C-CHO (100 mg, 0.074 mmol, 1.0 eq.) and 2-(5,6-difluoro-3-oxo-2,3-dihydro-1H-inden-1-ylidene) malononitrile (68 mg, 0.2 mmol, 4.0 eq.) in $CHCl_3$ (45 mL). The resulting mixture was stirred and heated to reflux for 12 h. After being cooled to room temperature, the solvent was removed under vacuum. The crude product was then purified by column chromatography on silica gel with PE/$CHCl_3$ (v/v = 1:1) as eluent to afford 7C-2F as a blue solid (116 mg, 88 %).^{1}H NMR (400 MHz, $CDCl_3$) δ 9.37 – 9.24 (m, 2H), 9.16 (d, *J* = 8.9 Hz, 2H), 8.55 (dd, *J* = 9.7, 6.5 Hz, 2H), 8.22 – 8.06 (m, 2H), 7.80 (t, *J* = 8.9 Hz, 2H), 7.71 (t, *J* = 7.5 Hz, 2H), 4.88 (dd, *J* = 15.7, 7.8 Hz, 4H), 3.32 – 3.22 (m, 4H), 2.32 – 2.14 (m, 2H), 1.91 (dd, *J* = 16.8, 8.0 Hz, 4H), 1.46 – 0.75 (m, 98H), 0.69 (dt, *J* = 19.5, 6.9 Hz, 14H). ^{13}C NMR (151 MHz, $CDCl_3$) δ 186.04, 185.90, 160.42, 158.13, 155.09, 153.64, 153.44, 153.33, 146.32, 144.08, 142.25, 141.28, 138.77, 138.35, 137.73, 136.40, 136.04, 135.92, 135.67, 134.73, 134.34, 134.24, 133.35, 133.21, 133.09, 132.98, 131.00, 129.78, 128.75, 127.15, 124.46, 120.11, 119.88, 119.61, 119.51, 118.08, 116.53, 114.84, 114.64, 114.36, 114.13, 112.45, 112.32, 68.77, 68.34, 56.00, 55.92, 39.48, 39.41, 31.89, 31.88, 31.86, 31.71, 31.65, 31.46, 31.37, 30.84, 30.78, 30.57, 30.02, 29.95, 29.92, 29.90, 29.84, 29.70, 29.64, 29.61, 29.58, 29.55, 29.50, 29.43, 29.34, 29.26, 25.90, 25.73, 25.63, 22.65, 22.63, 22.59, 22.54, 14.07, 14.06, 14.04, 14.02, 14.00. MS (MALDI-TOF) m/z: $[M + H]^+$ calculated for $C_{108}H_{125}F_4N_8O_2S_4$, 1770.8773, found: 1770.9161.

Compound 8C-CHO[2]

To a 100 mL flask, compound BTP-HD (200 mg, 0.167 mmol) and THF (20ml) were mixed under room temperature. Then powdery lithium aluminum hydride (127 mg, 20 eq.) was added to the mixture and the reactant was stirred at 80 ℃ overnight. After this, the mixture was poured into icy dilute hydrochloric acid solution and extracted three times with EA. The organic layer was washed with brine and dried over anhydrous

Na_2SO_4. After the solvent was evaporated, the intermediate diamine was obtained without further purification. The crude product was dissolved in acetic acid (CH_3CO_2H, 20 mL) and naphthalene-2,3-dicarbaldehyde (64 mg, 0.34 mmol, 2.0 eq.) were added to the solution in turn. The reaction was stirred at room temperature for 12 h, and the solvent was removed under vacuum. Finally, the residue was purified by column chromatography to give compound 8C-core as a yellow oil (187 mg, 85%). Under the protection of argon, $POCl_3$ (0.5 mL) was added to a solution of compound 8C-core (187 mg, 0.142 mmol) and DMF (1.0 mL) in DCE (20 mL). The resulting mixture was stirred and heated to reflux for 12 h, then was cooled to room temperature. The resulting mixture was slowly added into a saturated solution of sodium acetate (40 mL), then was stirred at room temperature for 2 h. The resulting mixture was extracted with DCM and the organic layer was dried over anhydrous Na_2SO_4. After removal of solvent, the crude product was purified by column chromatography on silica gel with PE/DCM (v/v = 2:1) as eluent to afford compound 8C-CHO as a yellow solid (181 mg, 93%). ^{1}H NMR (400 MHz, $CDCl_3$) δ 10.14 (s, 2H), 8.63 (s, 1H), 8.03 (s, 2H), 7.89 (d, *J* = 6.3 Hz, 1H), 7.61 – 7.46 (m, 2H), 5.80 – 5.60 (m, 2H), 4.62 (dd, *J* = 13.9, 7.6 Hz, 4H), 3.22 (t, *J* = 7.8 Hz, 4H), 1.96 (p, *J* = 7.6 Hz, 6H), 1.58 – 1.19 (m, 33H), 1.14 (q, *J* = 7.2 Hz, 5H), 1.08 – 0.81 (m, 42H), 0.81 – 0.61 (m, 20H). MS (MALDI-TOF) m/z: $[M + H]^+$ calculated for $C_{86}H_{122}N_4O_2S_4$, 1372.1880, found: 1372.3555.

Compound 8C-2F

Under the protection of argon, dry pyridine (0.2 mL) was added to a solution of compound 8C-CHO (90 mg, 0.066 mmol, 1.0 eq.) and 2-(5,6-difluoro-3-oxo-2,3-dihydro-1H-inden-1-ylidene) malononitrile (61 mg, 0.265 mmol, 4.0 eq.) in $CHCl_3$ (30 mL). The resulting mixture was stirred and heated to reflux for 12 h. After being cooled to room temperature, the solvent was removed under vacuum. The crude product was then purified by column chromatography on silica gel with PE/$CHCl_3$ (v/v = 1:1.5) as eluent to afford 8C-2F as a blue solid (109 mg, 92 %).^{1}H NMR (400 MHz, $CDCl_3$) δ 9.12 (d, *J* = 5.3 Hz, 2H), 8.55 (dt, *J* = 9.9, 6.9 Hz, 3H), 8.05 (d, *J* = 22.6 Hz, 2H), 7.92 (dd, *J* = 6.1, 3.5 Hz, 1H), 7.69 (td, *J* = 7.5, 4.6 Hz, 2H), 7.60 (dt, *J* = 6.3, 3.4 Hz, 2H),

5.71 (s, 2H), 4.75 (dd, *J* = 18.2, 7.6 Hz, 4H), 3.21 (t, *J* = 9.7 Hz, 4H), 2.07 (s, 2H), 1.88 (q, *J* = 8.4, 8.0 Hz, 4H), 1.66 – 1.46 (m, 9H), 1.46 – 0.90 (m, 73H), 0.90 – 0.61 (m, 28H). ^{13}C NMR (151 MHz, $CDCl_3$) δ 186.05, 158.79, 158.71, 155.09, 154.22, 153.35, 145.80, 143.35, 139.04, 138.93, 138.71, 136.98, 136.80, 136.59, 135.14, 134.88, 134.42, 133.51, 133.33, 131.72, 131.31, 129.88, 128.99, 128.08, 126.94, 122.84, 119.59, 119.13, 115.09, 115.03, 114.80, 114.67, 112.43, 112.30, 112.18, 68.20, 67.77, 55.37, 39.00, 38.92, 31.93, 31.92, 31.90, 31.71, 31.41, 31.38, 30.62, 30.57, 30.55, 29.96, 29.89, 29.84, 29.75, 29.72, 29.68, 29.65, 29.60, 29.58, 29.55, 29.53, 29.49, 29.45, 29.39, 29.37, 29.31, 29.25, 25.65, 25.57, 25.53, 22.70, 22.69, 22.64, 22.62, 22.58, 22.53, 14.13, 14.10, 14.08, 14.07. MS (MALDI-TOF) m/z: $[M - H]^+$ calculated for $C_{110}H_{125}F_4N_8O_2S_4$, 1793.8744, found: 1793.9273.

2. Measurements and Characterizations

The ^{1}H and ^{13}C NMR spectra were taken on a Bruker AV400 Spectrometer. Matrix assisted laser desorption/ionization time-of-flight (MALDI-TOF) mass spectrometry were performed on a Bruker Auto flex III instrument. Varian 7.0T FTMS was used to achieve the HRMS data. UV-vis spectra were obtained with a UV-VIS-NIR spectrophotometer (SHIMADZU, UV-3600). Cyclic voltammogram (CV) was performed with a LK2010 Microcomputer based Electrochemical Analyzer at a scan rate of 100 mV/s. Thermogravimetric analyses (TGA) were carried out on a NETZSCH STA 449 F5 Jupiter instrument under a purified nitrogen gas. The heating rate is a 10 °C/ min heating rate. The current density-voltage (*J-V*) curves of photovoltaic devices were obtained by a Keithley 2400 source-measure unit. The photocurrent was measured under simulated illumination of 100 mW cm^{-2} with AM 1.5 G irradiation using a xenon-lamp-based solar simulator [Oriel 96000] in an argon-filled glove box. EQEs of the encapsulated devices were obtained with a halogen-tungsten lamp, monochromator, optical chopper, and lock-in amplifier in air and the photon flux was determined by a calibrated silicon photodiode. Atomic force microscopy (AFM) images were performed using in tapping mode on a Bruker Multi Mode 8 atomic force microscope. Transmission electron microscopy (TEM) was performed on a Philips Technical G2

F20 at 200 kV. The GIWAXS (grazing incidence wide angle X-ray scattering) samples were prepared on ZnO-coated Si substrates using the same preparation conditions as for devices and All samples were deposited on the silicon and were irradiated at a fixed X-ray incident angle of 0.200° with an exposure time of 16 s. The hole and electron mobility were measured using the space charge limited current (SCLC) method, employing a diode configuration of ITO/PEDOT:PSS/active layer/MoO_x/Ag for hole and glass/ITO/ZnO/active layer/PDINN/Al for electron by taking the dark current density in the range of 0–10 V and fitting the results to a space charge limited form, where SCLC is described by:[3]

$$J = \frac{9\varepsilon_r\varepsilon_0\mu V^2}{8L^3}$$

where J is the current density, L is the film thickness of the active layer, μ is the hole or electron mobility, ε_r is the relative dielectric constant of transport medium, ε_0 is the permittivity of free space (8.85×10^{-12} F m^{-1}), V (= V_{appl} -V_{bi}) is the internal voltage in the device, where V_{appl} is the applied voltage to the device and V_{bi} is the built-in voltage due to the relative work function difference of the two electrodes. The hole and electron mobility of the solar cell blend are deduced from the intercept value of $9\varepsilon_0\varepsilon_r\mu/(8L^3)$ by linearly plotting ln(J) *vs*. ln(V) (the slope of ln(J) vs. ln(V) is ≈ 2).

The current density-voltage (*J*-*V*) characteristics of photovoltaic devices were obtained using a Keithley 2400 source-measure unit. The photocurrent was measured under illumination simulated 100 mW cm^{-2} AM1.5G irradiation using SAN-EI XES-70S1 solar simulator, calibrated with a standard Si solar cell. The EQE spectrum was measured using a QE-R Solar Cell Spectral Response Measurement System (Enli Technology Co., Ltd., Taiwan).

For the transient photocurrent (TPC) and transient photovoltage (TPV) measurements, the device was mounted on a conductive clip and under steady-state illumination from focused Quartz Tungsten-Halogen Lamp light source. The measurements were performed with background response similar to open-circuit voltage. An optical perturbation is applied to the device with a 1 kHz femtosecond pulse laser under 450 nm excitation. The TPV signal was acquired by a digital oscilloscope at open-circuit

condition. TPC signal was measured under approximately short-circuit condition by applying a 50 Ω resistor. The photovoltage decay kinetics of all devices follow a mono-exponential decay: $\delta V = A\exp(-t/\tau)$, where t is the time and τ is the charge carrier lifetime. EQE_{EL} measurements were done from 0.01 V to 2.5 V using a home built setup using a Keithley 2400 to inject current to the solar cells. Emission photon-flux from the solar cells was recorded using a Si detector (Hamamatsu s1337-1010BQ) and a Keithley 6482 picoammeter. FTPS-EQE measurements were done from 500 nm to 1300 nm using a halogen lamp light source, chopped at a frequency of 173 Hz, a monochromator (Newport CS260), a Stanford SR830 lock-in amplifier, a Stanford SR570 current amplifier, and a set of long pass filters. Lamp intensity was calibrated using a Si detector (Hamamatsu s1337-1010BQ).

3. DFT calculation

The molecular geometries were optimized by Gaussian 09 with a functional of B3LYP and a basis set of 6-31G(D). The dipole moment calculation type was carried out in FOPT.

4. Fabrication and characterization of OSCs

The structure of all OSCs adopt the conventional device structure, namely ITO/PEDOT:PSS/active layer/PDINN/Ag structure. The pre-patterned ITO glass substrates are sonicated with deionized water twice (with detergent and without detergent), acetone and isopropanol sequentially in an ultrasonic bath. Before use, these glasses are dried in a vacuum oven and treated by UV-ozone for 30 mins to improve its work function and clearance. Immediately, the PEDOT:PSS aqueous solution (Baytron P 4083, from HCStarck) is filtered by a 0.45 mm filter and pre-coated onto these pre-cleaned ITO glasses at 5000 rpm for 30 seconds. Then heat the ITO to dry it at 150 ℃ for 20 mins in air. The PEDOT:PSS coated ITO substrates were transferred to a N_2-filled glove box for further processing. The optimized recipes for device fabrication

were D:A weight ratio of 1:1.2, solution concentration of 13.2 mg/ml in $CHCl_3$ with 0.5% 1-chloronaphthalene as additive. Then the solution was stirred for 2 hours for intensive mixing. The blend solutions were spin-coated on the PEDOT:PSS transport layer at 3000 rpm for 30 seconds, then annealed at 80 °C for 10 minutes. After cooling to room temperature, the PDINN methanol solution with a concentration of 1.0 mg mL^{-1} was deposited on these active layers at 5000 rpm for 30 seconds. Then, an Ag layer (~100 nm) was deposited in thermal evaporator under vacuum of 5×10^{-5} Pa through a shadow mask. The active area of the OSCs was 4.5 mm^2, which was defined by Optical microscope (Olympus BX51).

5. Supplementary Figures

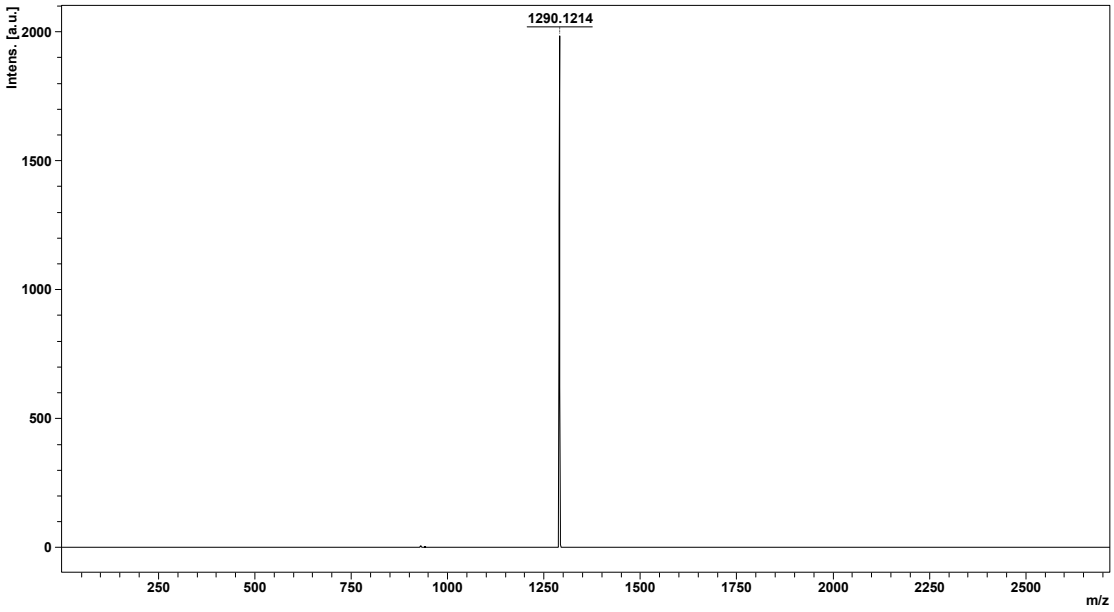

Fig. S1 MS (MALDI-TOF) spectrum of 6C-core.

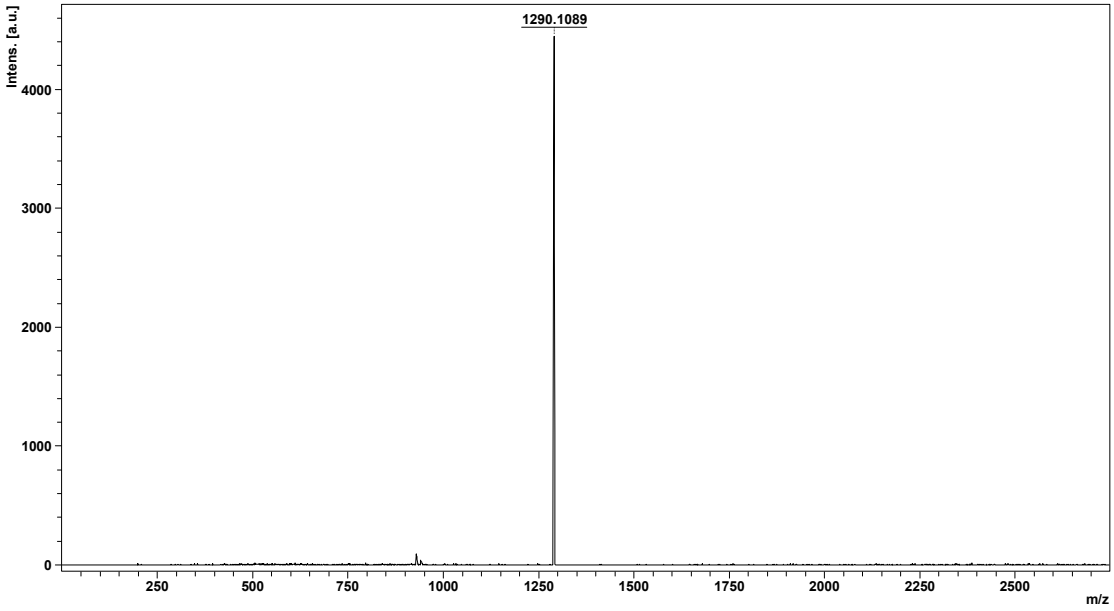

Fig. S2 MS (MALDI-TOF) spectrum of 7C-core.

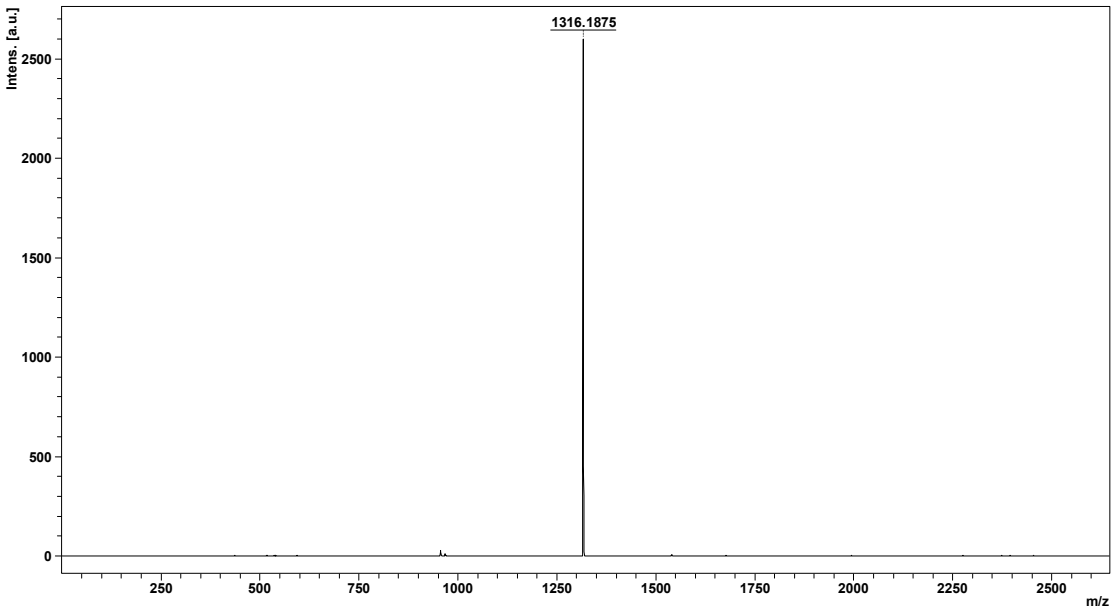

Fig. S3 MS (MALDI-TOF) spectrum of 8C-core.

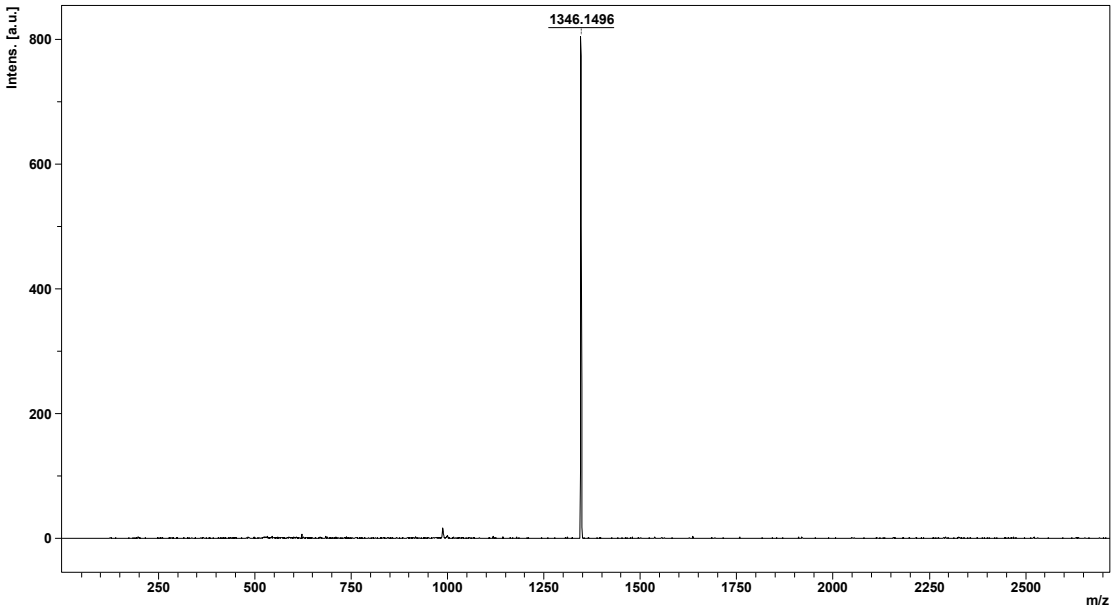

Fig. S4 MS (MALDI-TOF) spectrum of 6C-CHO.

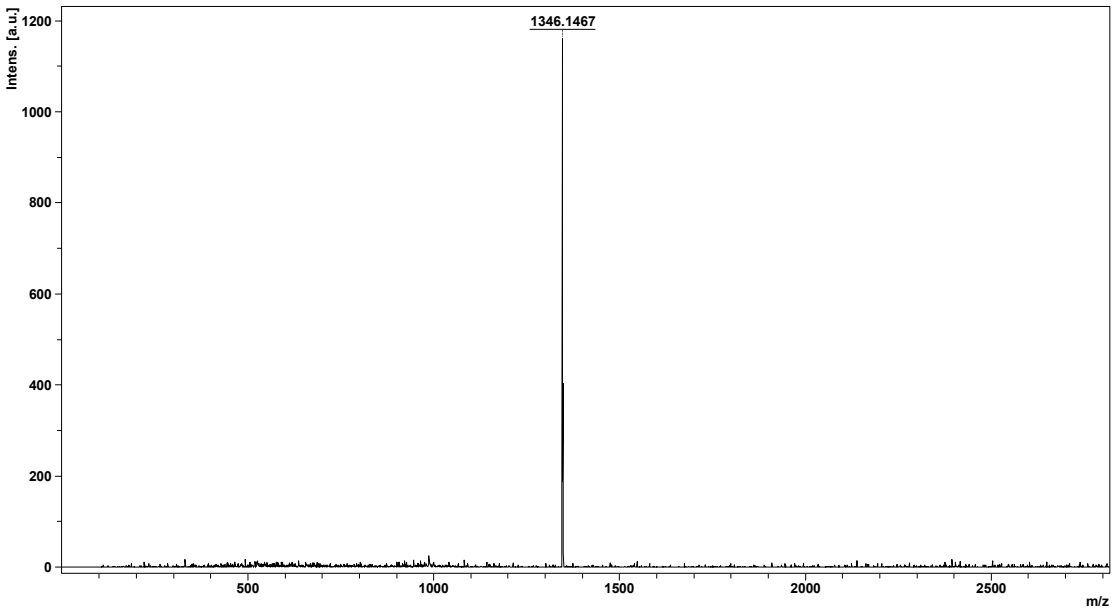

Fig. S5 MS (MALDI-TOF) spectrum of 7C-CHO.

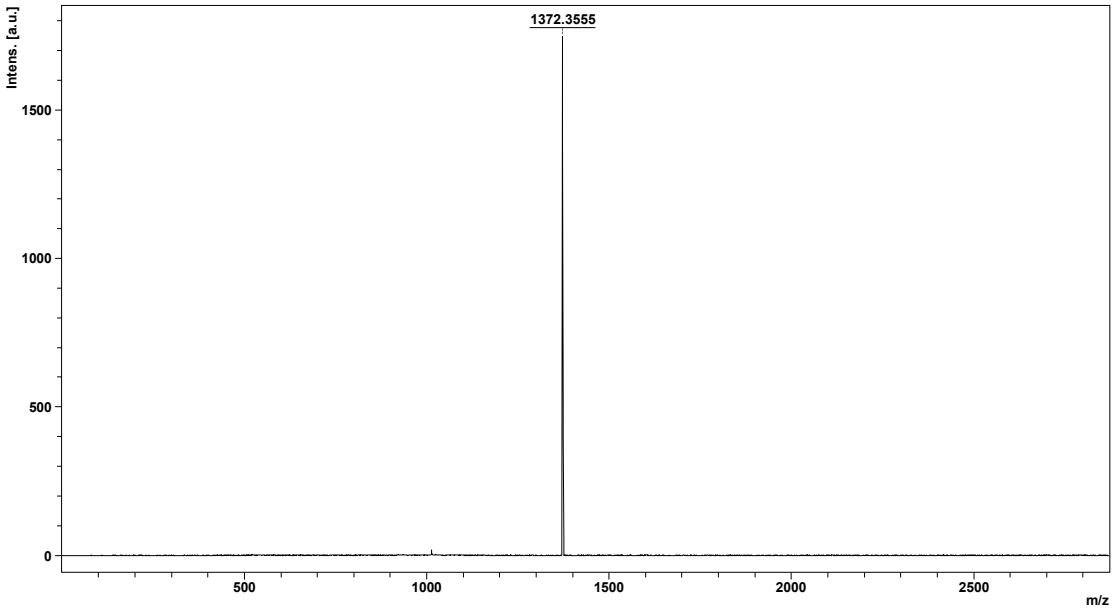

Fig. S6 MS (MALDI-TOF) spectrum of 8C-CHO.

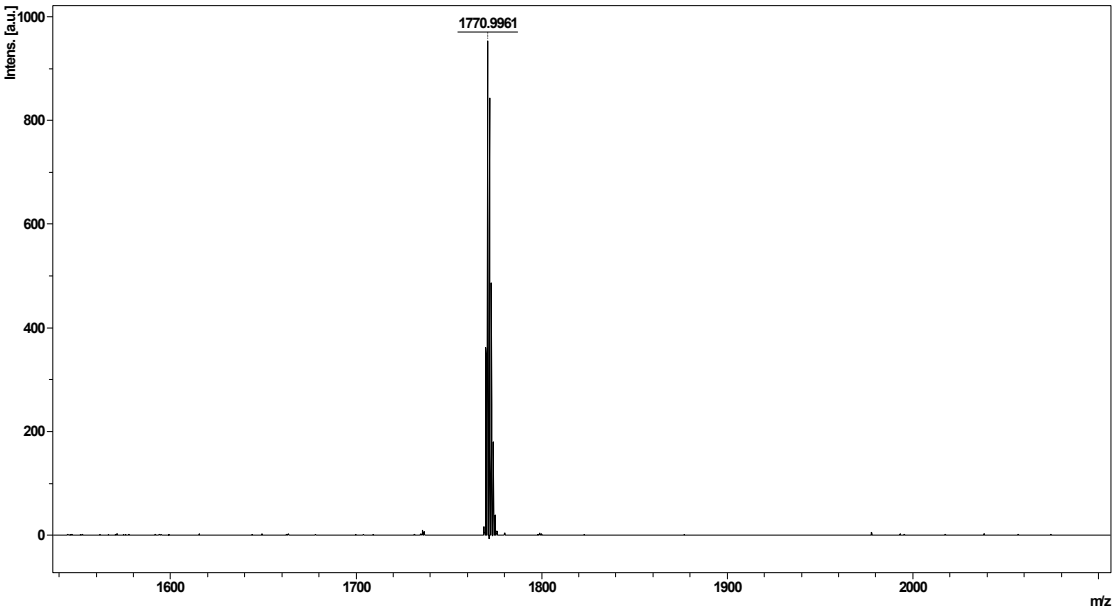

Fig. S7 MS (MALDI-TOF) spectrum of 6C-2F.

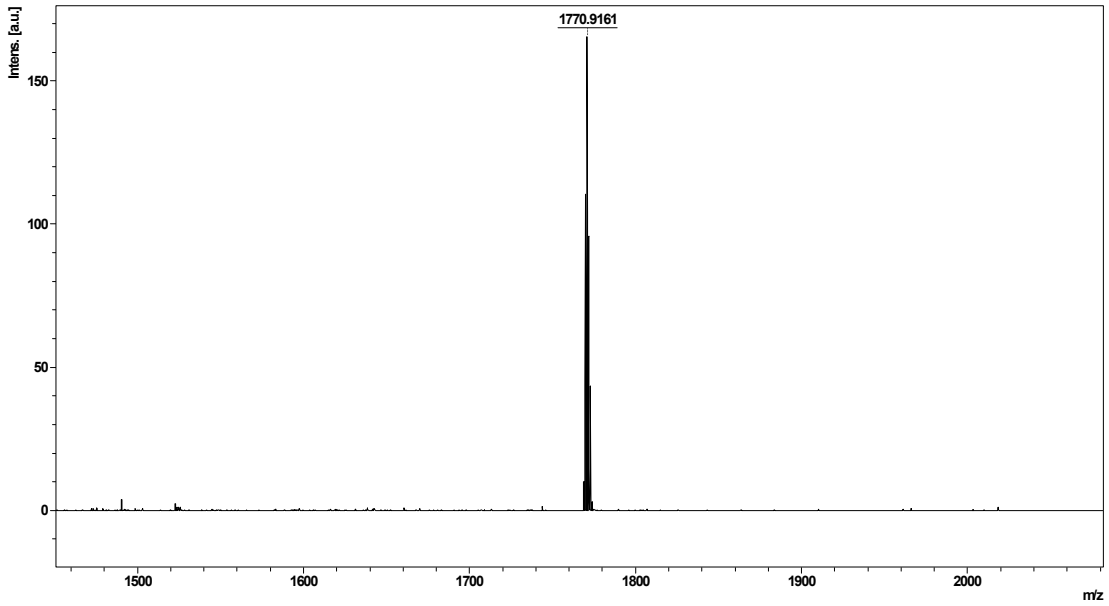

Fig. S8 MS (MALDI-TOF) spectrum of 7C-2F.

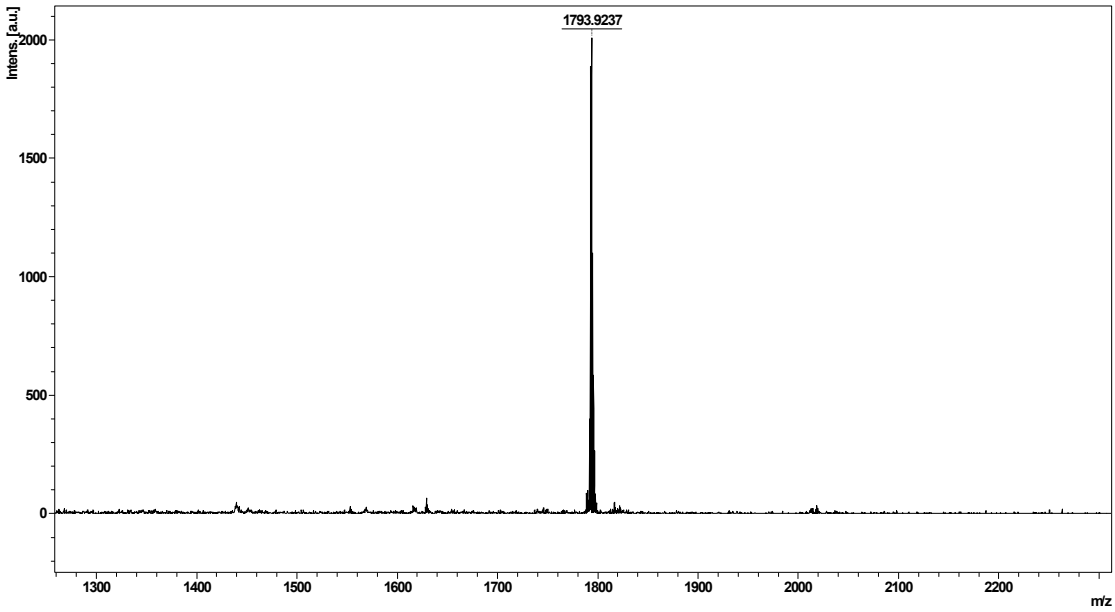

Fig. S9 MS (MALDI-TOF) spectrum of 8C-2F.

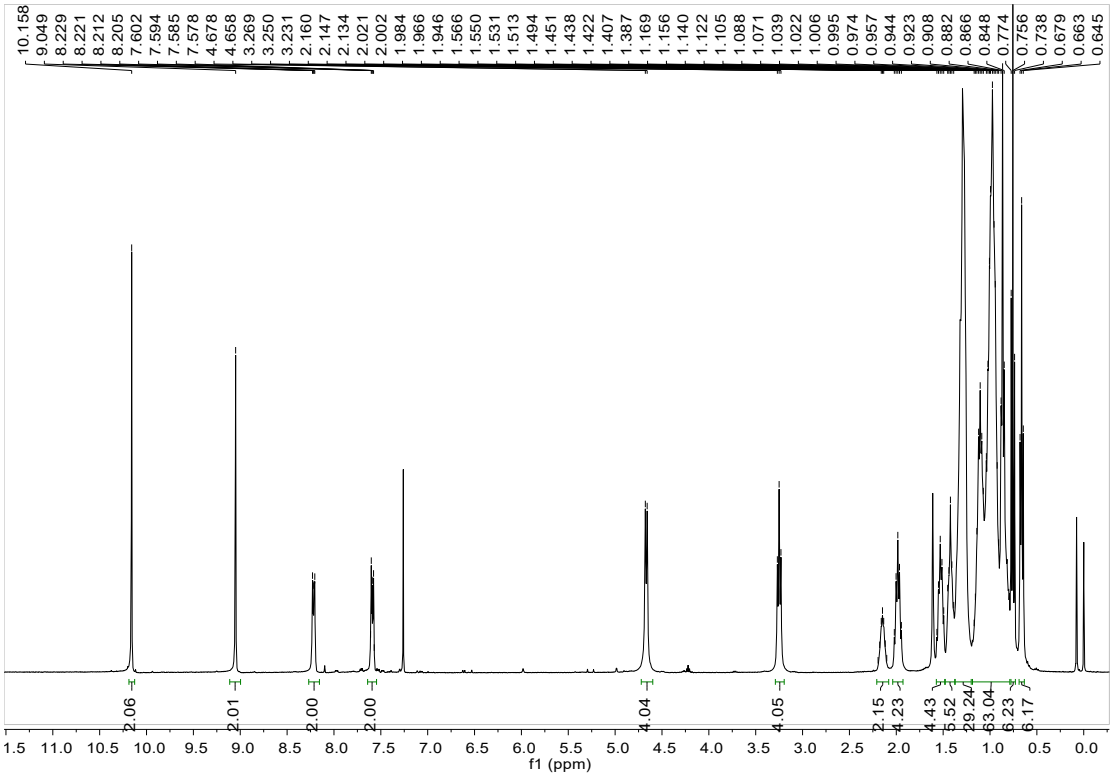

Fig. S10 ^{1}H NMR spectrum of compound 6C-CHO in $CDCl_3$.

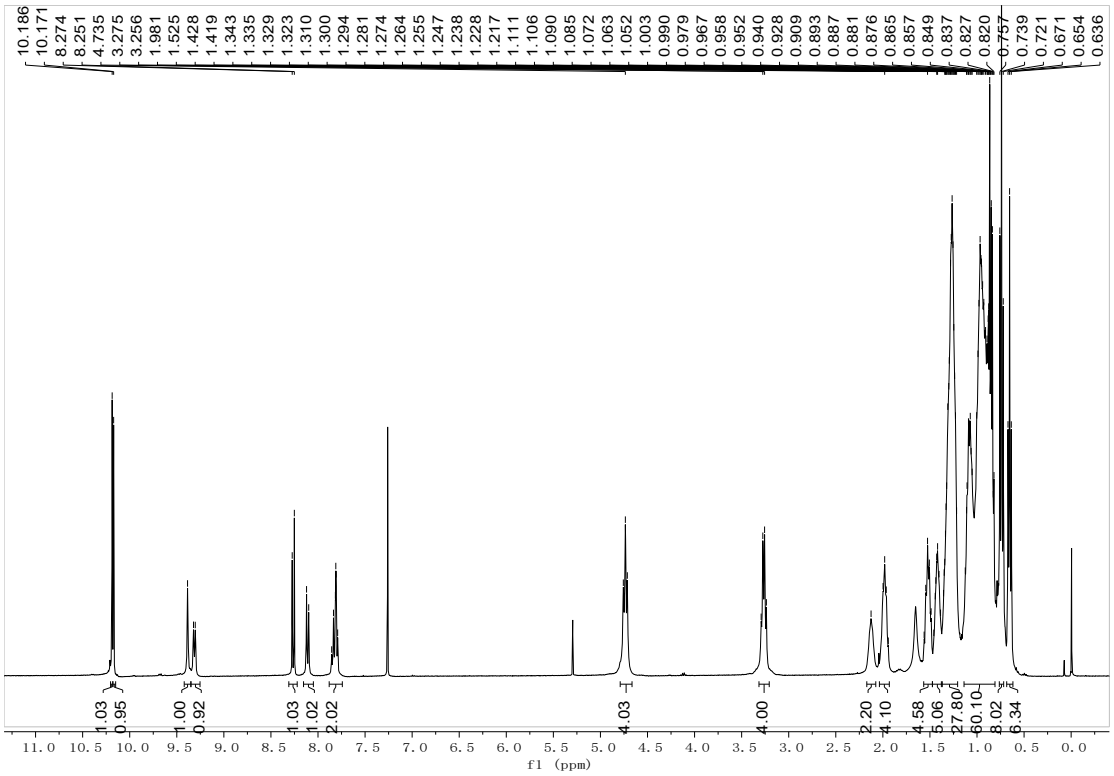

Fig. S11 ^{1}H NMR spectrum of compound 7C-CHO in $CDCl_3$.

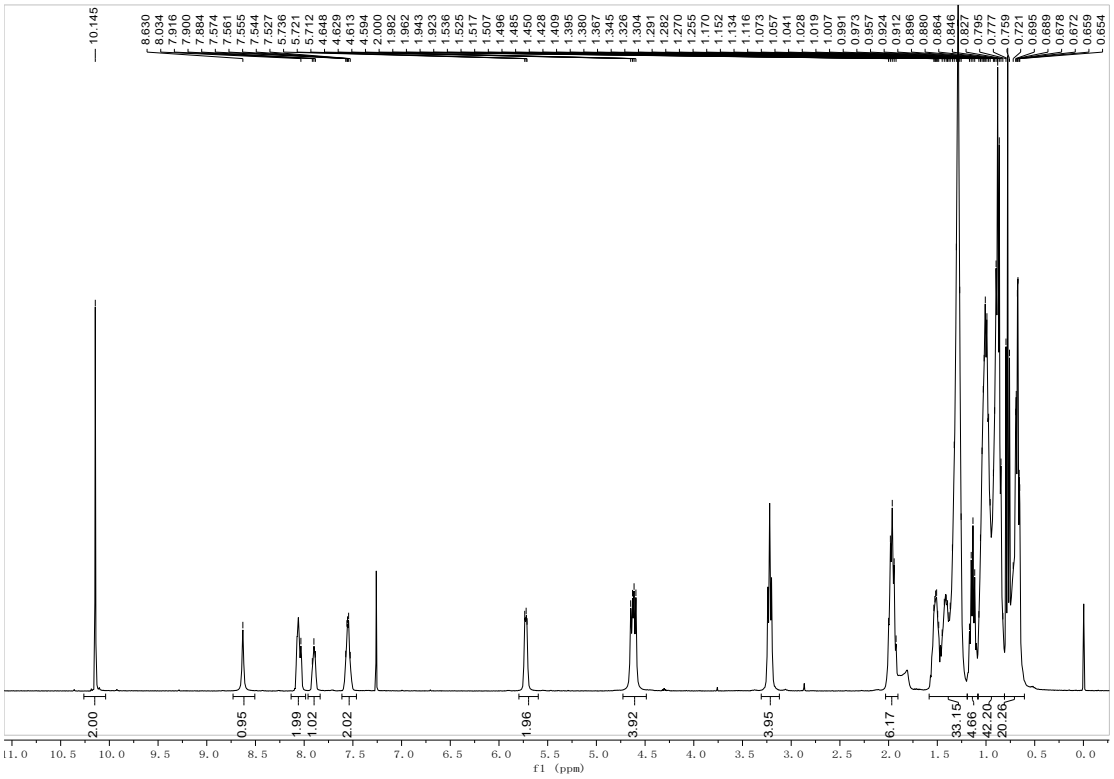

Fig. S12 ^{1}H NMR spectrum of compound 8C-CHO in $CDCl_3$.

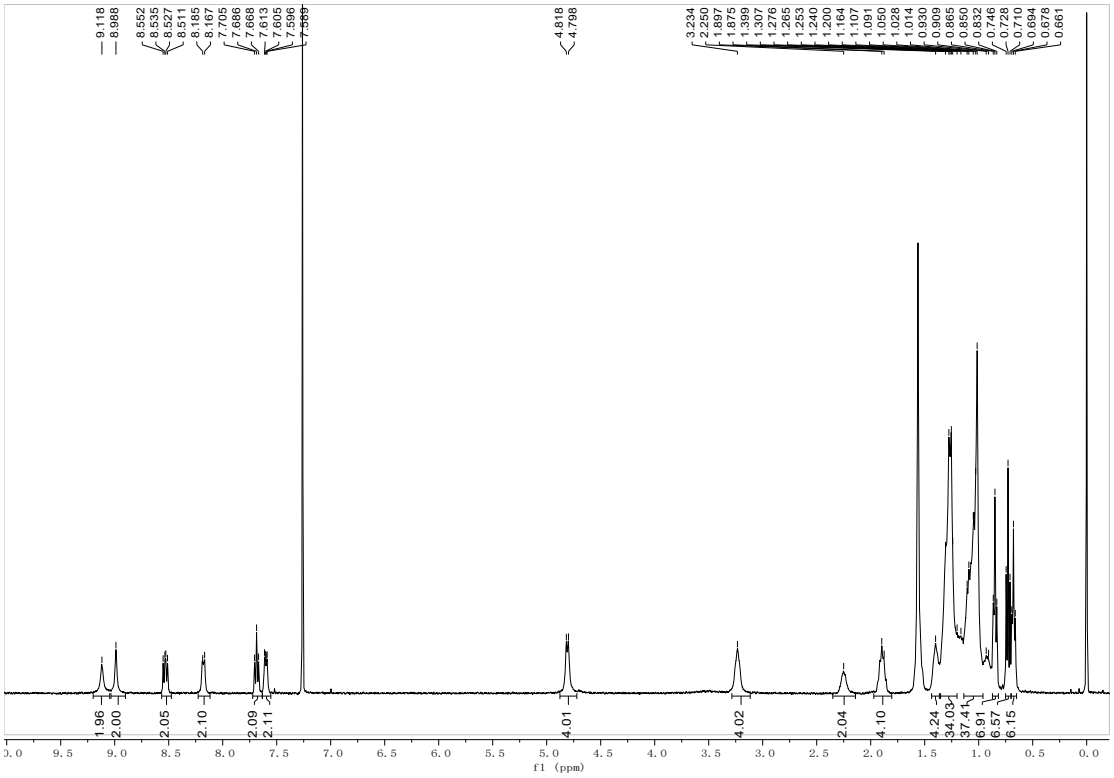

Fig. S13 ^{1}H NMR spectrum of compound 6C-2F in $CDCl_3$.

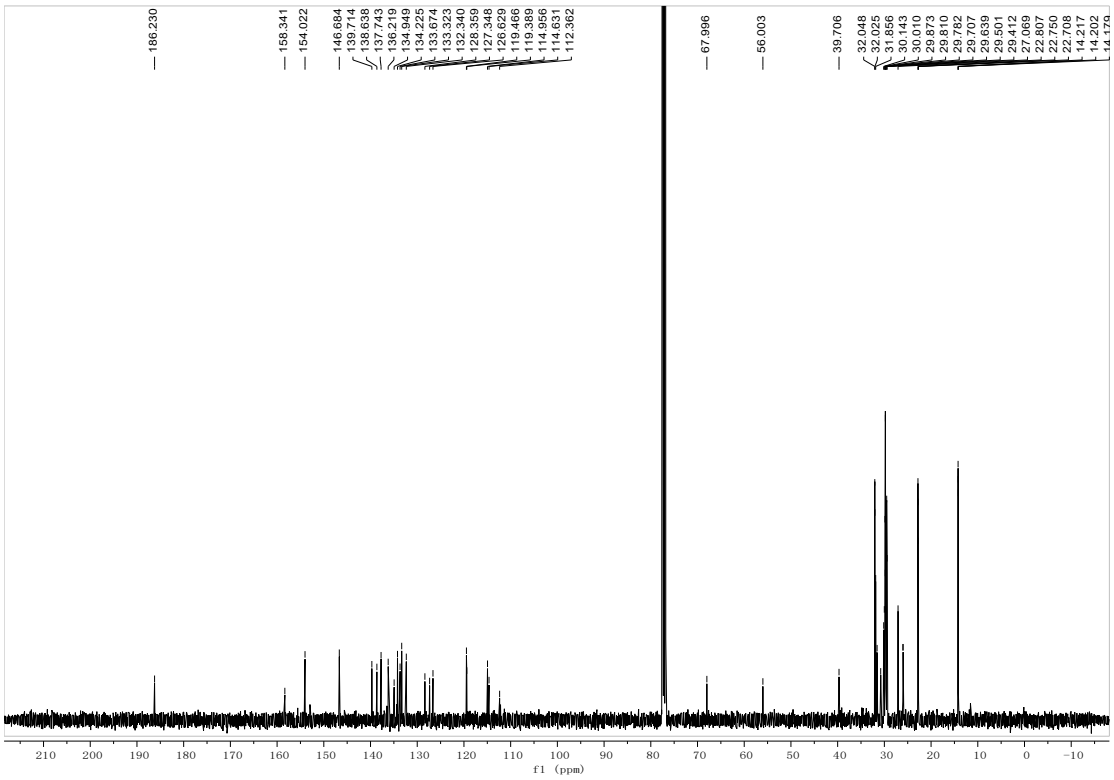

Fig. S14 ^{13}C NMR spectrum of compound 6C-2F in $CDCl_3$.

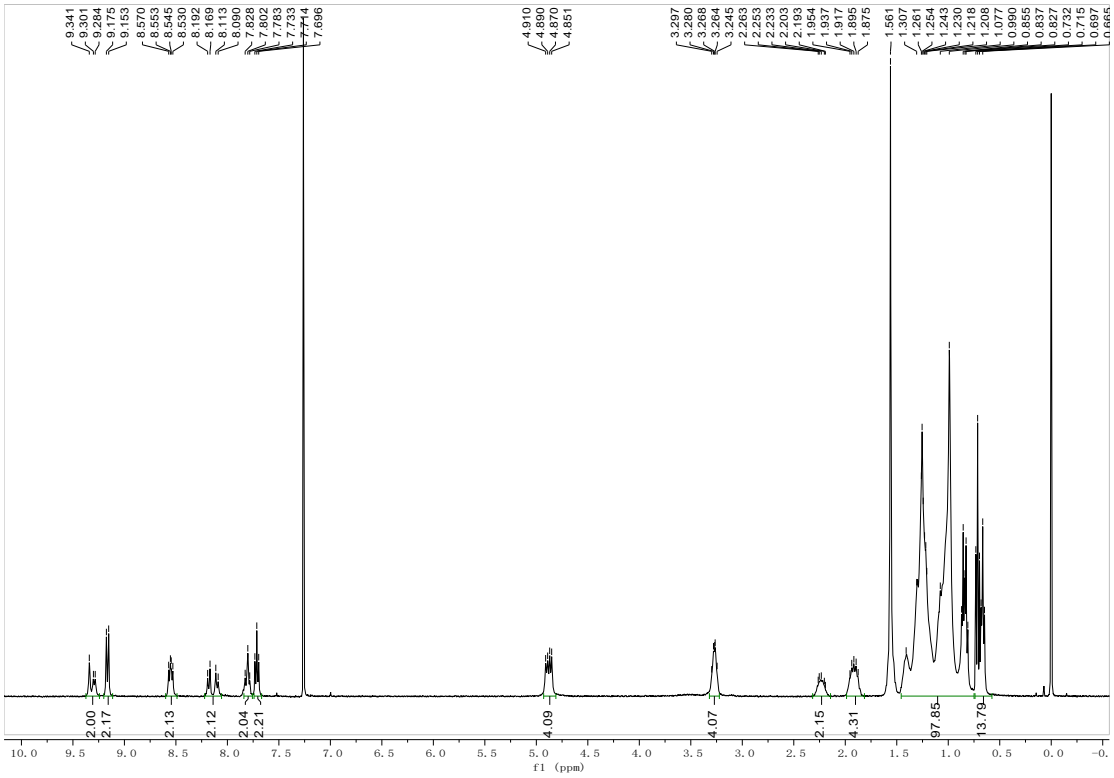

Fig. S15 ^{1}H NMR spectrum of compound 7C-2F in $CDCl_3$.

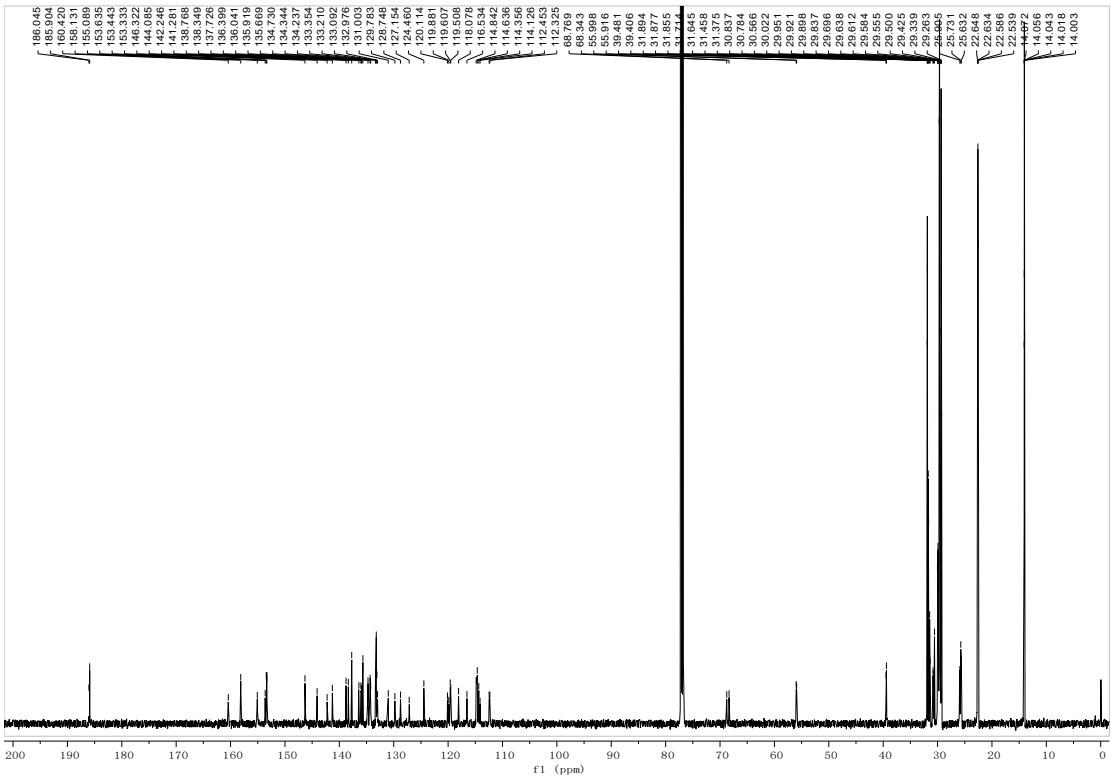

Fig. S16 ^{13}C NMR spectrum of compound 7C-2F in $CDCl_3$.

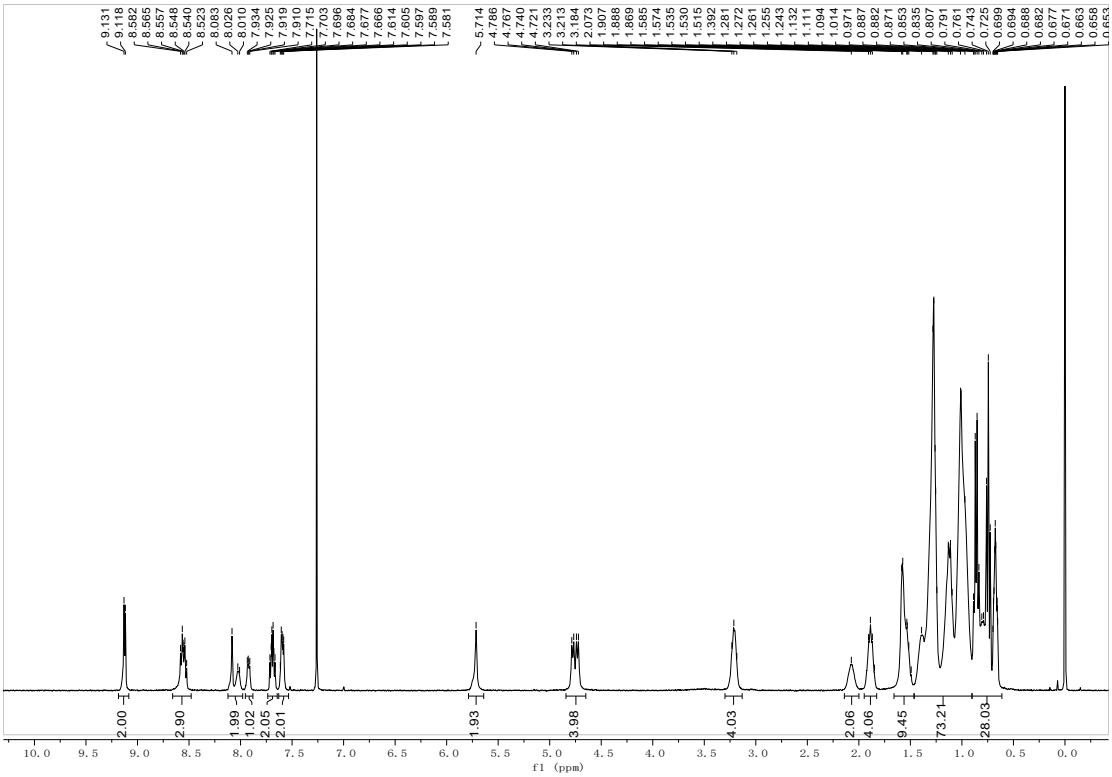

Fig. S17 ^{1}H NMR spectrum of compound 8C-2F in $CDCl_3$.

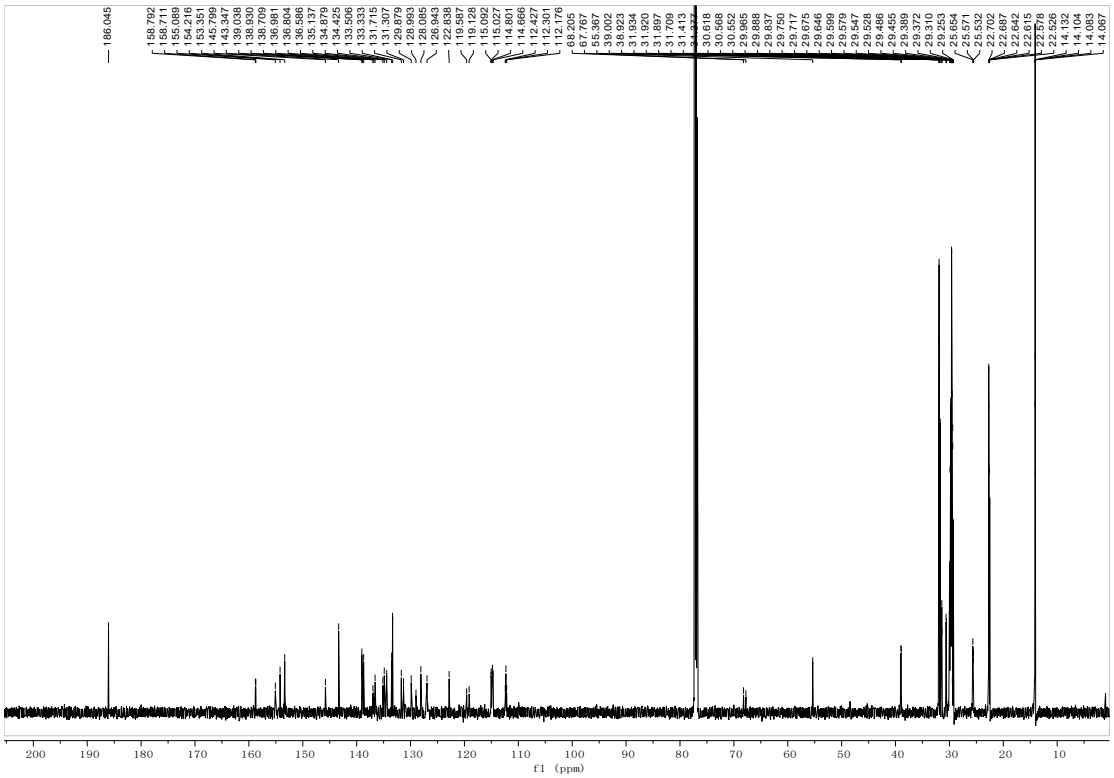

Fig. S18 ^{13}C NMR spectrum of compound 8C-2F in $CDCl_3$.

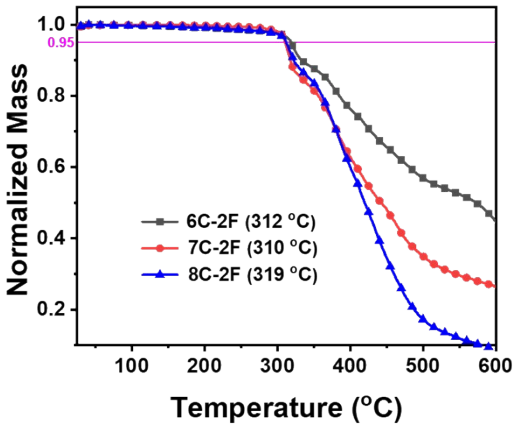

Fig. S19 Thermal gravimetric analysis curve of acceptors 6C-2F, 7C-2F and 8C-2F.

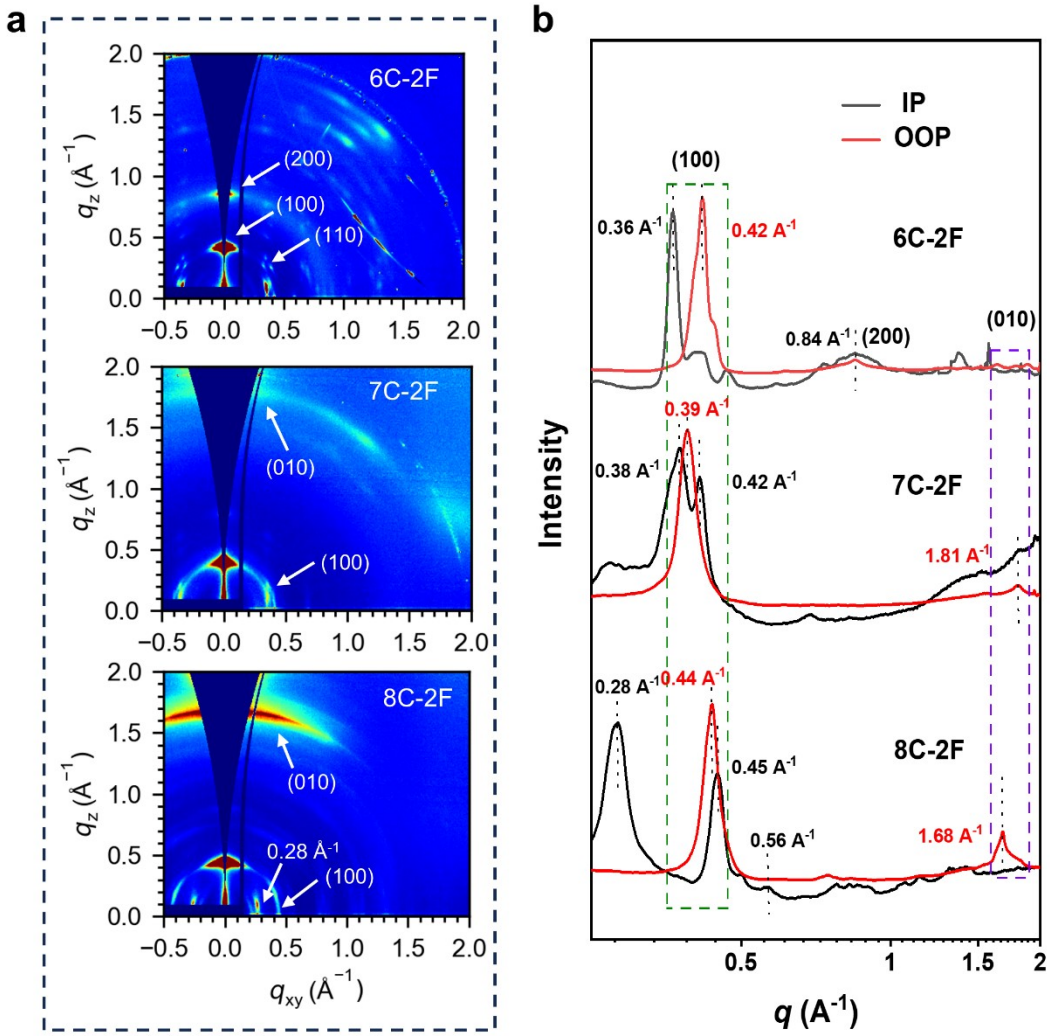

Fig. S20 (a) 2D GIWAXS diffraction images of pristine films. (b) The IP and OOP extracted line-cut profiles of pristine films.

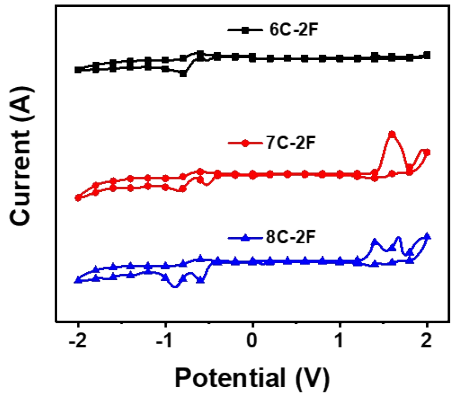

Fig. S21 Cyclic voltammograms of acceptors 6C-2F, 7C-2F and 8C-2F in thin films.

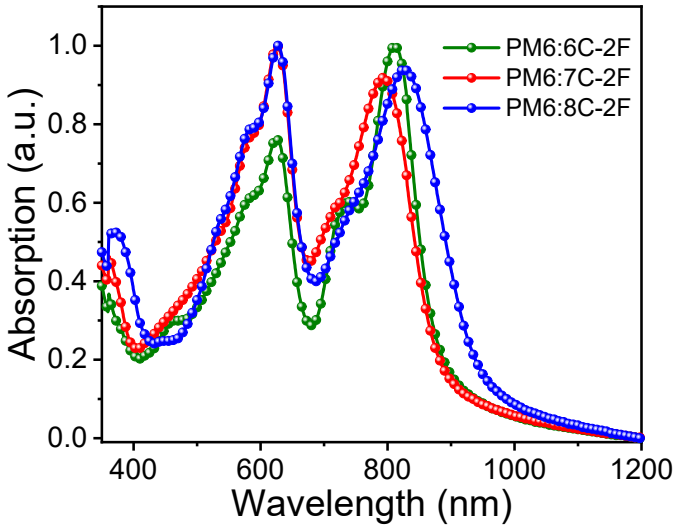

Fig. S22 Normalized absorption spectra of three BHJ blends based on PM6:6C-2F, PM6:7C-2F and PM6:8C-2F.

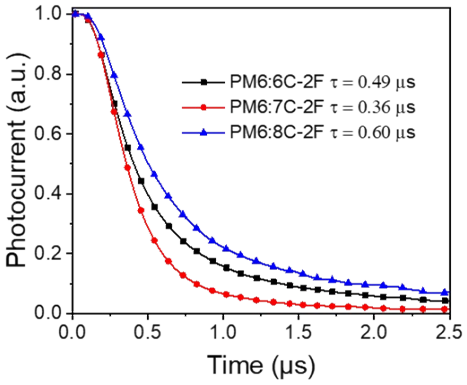

Fig. S23 Transient photocurrent measurements of the optimized devices.

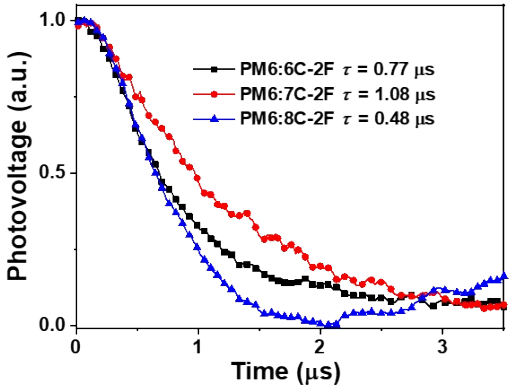

Fig. S24 Transient photovoltage measurements of the optimized devices.

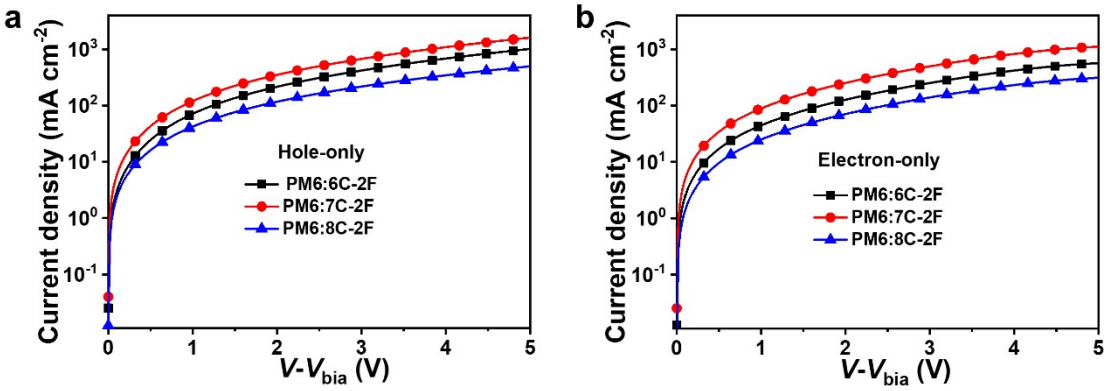

Fig. S25 (**a**) The hole and (**b**) electron mobility of PM6:6C-2F, PM6:7C-2F and PM6:8C-2F blend films measured by SCLC method.

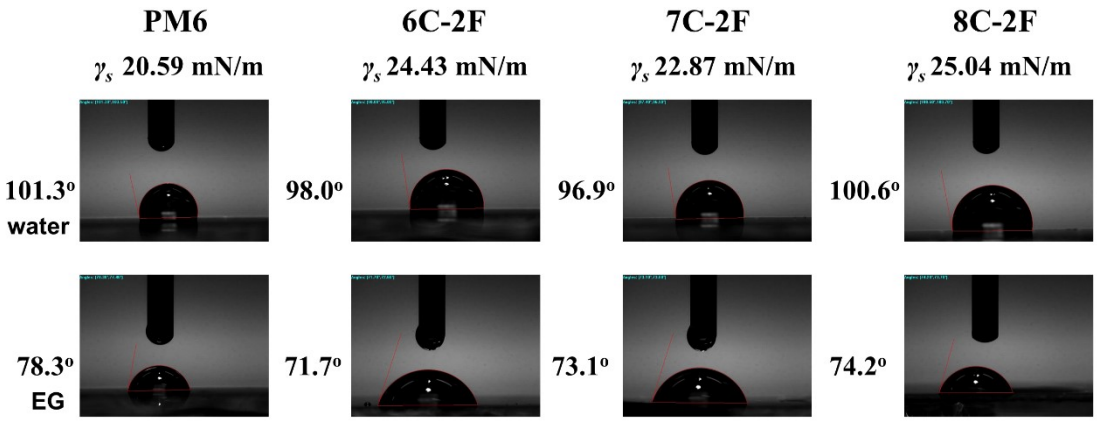

Fig. S26 Contact angles and surface free energies of donor PM6 and SMAs 6C-2F, 6C-2F, 6C-2F pristine films.

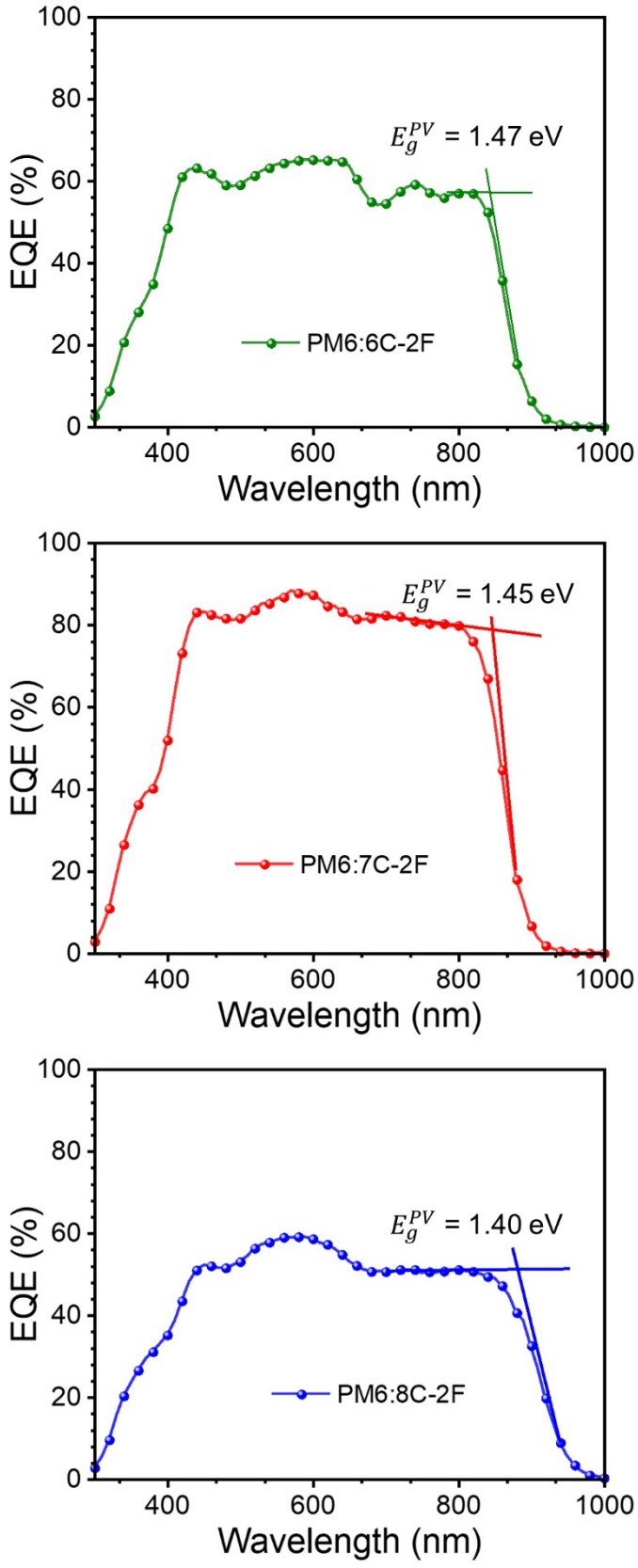

Fig. S27 The calculated energy gaps of OSCs based on PM6:6/7/8C-2F from their EQE spectra.

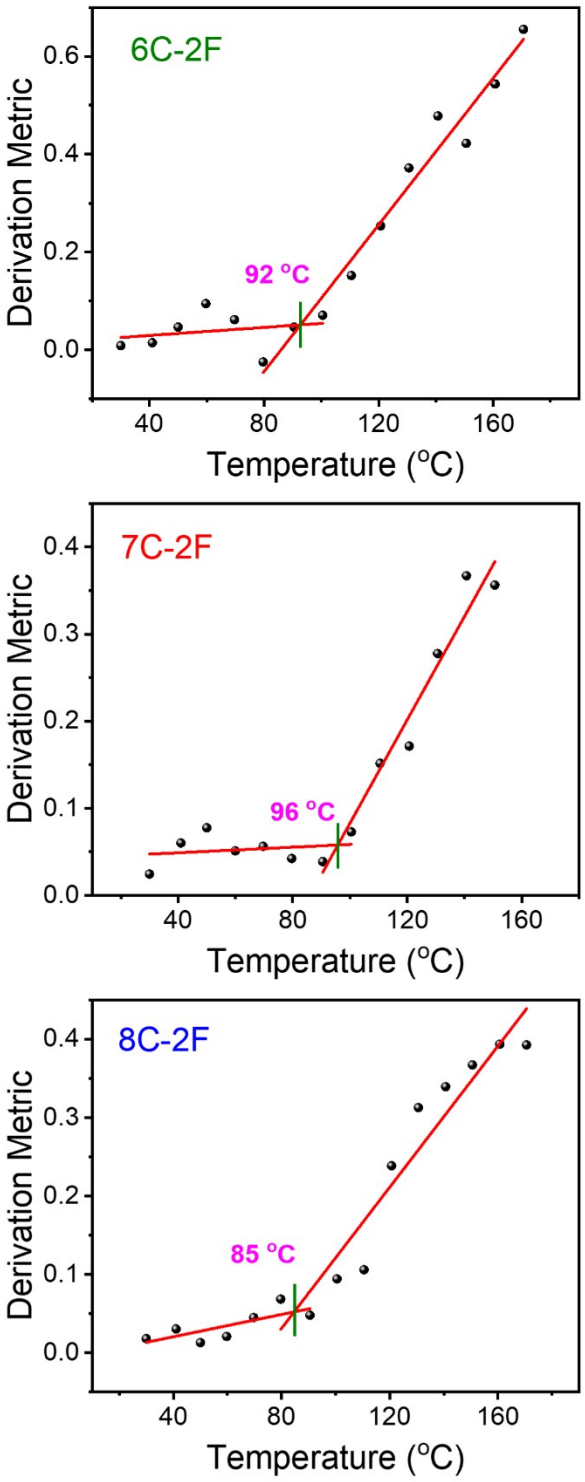

Fig. S28 Glass transition temperature T_gs of 6C-2F, 7C-2F and 8C-2F obtained from UV-vis deviation metric results.

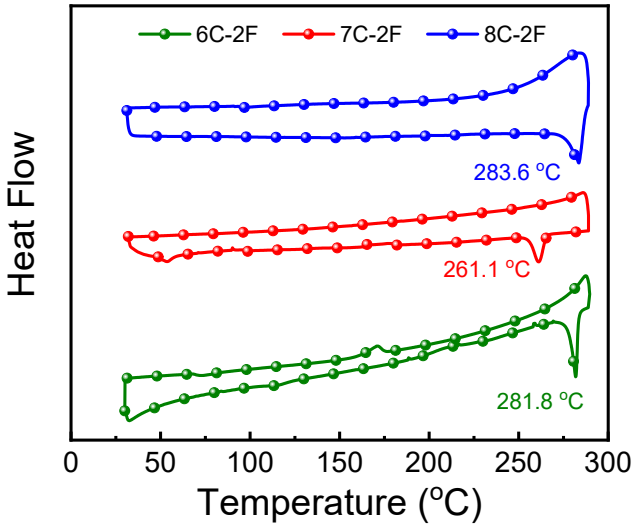

Fig. S29 DSC heating curves for three NFAs 6/7/8C-2F with the speed of 10 °C/min.

6. Supplementary Tables

Table S1 Summary of the GIWAXS parameters for neat and blend films

Film	q (010, A^{-1})	$d_{\pi-\pi}$ (010, A)	CCL (010, A)	q (100, A^{-1})	d_{L-L} (100, A)	CCL (010, A)
6C-2F	---	--	--	0.365	17.3	380.1
7C-2F	1.81	3.47	70.3	0.376	16.7	206.3
8C-2F	1.68	3.74	67.4	0.437	14.4	66.4
PM6:6C-2F	1.78	3.53	107.0	0.293	21.4	149.1
PM6:7C-2F	1.73	3.63	28.7	0.291	21.6	107.1
PM6:8C-2F	1.71	3.67	34.9	0.288	21.8	97.0

Table S2 Detailed data of the hole mobility and electron mobility.

Active layers	μ_h (cm^2 v^{-1} s^{-1})	μ_e (cm^2 v^{-1} s^{-1})	Ratio
PM6:6C-2F	6.3×10^{-5}	2.7×10^{-5}	2.3
PM6:7C-2F	4.2×10^{-4}	3.7×10^{-4}	1.1
PM6:8C-2F	4.6×10^{-5}	1.9×10^{-5}	2.4

Table S3 Contact angles and surface energy parameters of pristine films. [a]

Film	θ_{H2O} [°]	θ_{EG} [°]	γ^d [mN m^{-1}]	γ^p [mN m^{-1}]	γ^a [mN m^{-1}]	$\chi^{D\text{-}A}$ [b]
PM6	101.3	78.3	19.04	1.55	20.59	--
6C-2F	98.0	71.7	22.83	1.60	24.43	0.164
7C-2F	96.9	73.1	20.56	2.31	22.87	0.060
8C-2F	100.6	74.2	24.15	0.90	25.04	0.218

[a]The γ^d and γ^p represent the surface free energies generated from the dispersion force and polar force, respectively.[4]

Table S4 Statistical sheet of binary devices based on PM6:Y-series active layers.

Acceptor	V_{oc} [V]	J_{sc} [mA cm^{-2}]	FF [%]	PCE [%]	Ref.
Y6	0.83	25.3	74.8	15.7	5
CH-BBQ	0.881	26.15	78.9	18.19	6
Ch-iBQ	0.879	26.04	78.5	17.97	6
CH-BQ	0.84	23.61	64.8	12.85	6
ZCCF3	0.88	12.40	64.2	6.99	7
AQx-1	0.893	22.18	67.14	13.31	8
AQx-2	0.86	25.38	76.25	16.64	9
Y18	0.84	25.71	76.5	16.52	10
Y6-Se	0.82	25.47	75	15.82	11
Y6-2Se	0.83	24.32	70	14.62	11
CH17	0.883	26.19	77.2	17.84	1
CH20	0.881	25.44	74.92	16.79	12
CH21	0.873	26.57	78.13	18.12	12
CH22	0.884	26.74	80.62	19.06	12
YB2T	0.918	24.48	75.85	17.05	13
YB2B	0.953	19.30	59.46	10.94	13
NQF	0.921	25.79	73.96	17.57	14
CH45	0.910	25.57	78.0	18.15	15
CH4	0.908	24.67	66.4	14.87	15
Qx-1	0.911	26.1	75.5	17.9	16
Qx-2	0.934	26.5	73.7	18.2	16
CB16	0.92	25.98	76.89	18.32	17
BQx	0.892	26.11	72.8	17.0	18
BQx-CN	0.880	26.77	79.7	18.8	18

BQx-2CN	0.863	25.90	77.2	17.3	18
BZ-C4	0.882	25.69	74.63	16.89	19
BZ-E22	0.873	26.39	75.84	17.46	19
BZ-E31	0.875	27.31	76.72	18.33	19
BZ-E62	0.879	25.98	75.17	17.15	19
6C-2F	**0.914**	**19.15**	**61.90**	**10.83**	**This work**
8C-2F	**0.840**	**18.57**	**52.16**	**8.13**	**This work**
7C-2F	**0.900**	**26.71**	**78.33**	**18.83**	**This work**

Table S5. Photovoltaic parameters of the optimized devices based on PM6:6/7/8C-2F with D:A ratio of 1:1.2 and liquid additive CN but different electron transport layer (ETL).

ETL	Active layers	V_{oc} [V]	J_{sc}[mA cm^{-2}]	FF [%]	PCE [%]
F3N	PM6:6C-2F	0.912	17.50	61.52	9.83
	PM6:7C-2F	0.911	25.76	76.75	18.00
	PM6:8C-2F	0.825	17.94	51.67	7.64
PDINN	PM6:6C-2F	0.910	18.73	60.45	10.31
	PM6:7C-2F	0.907	26.54	75.48	18.18
	PM6:8C-2F	0.831	18.19	51.35	7.77

Table S6. Photovoltaic parameters of the optimized devices based on PM6:6/7/8C-2F with D:A ratio of 1:1.25 and PDINN as the ETL but different ratios of additive 1-chloro-4-iodobenzene (CIB).

Active layer	CIB ratios	V_{OC} [V]	J_{sc}[mA cm^{-2}]	FF [%]	PCE [%]
PM6:6C-2F	50%	0.914	19.34	60.26	10.61
PM6:7C-2F		0.898	26.49	76.80	18.28
PM6:8C-2F		0.833	18.19	52.84	8.01
PM6:6C-2F	75%	0.914	19.15	61.90	10.83
PM6:7C-2F		0.900	26.71	78.33	18.83
PM6:8C-2F		0.840	18.57	52.16	8.13

PM6:6C-2F		0.914	18.83	61.72	10.63
PM6:7C-2F	100%	0.898	26.69	77.08	18.48
PM6:6C-2F		0.837	18.66	51.59	8.06

Reference

1. H. Chen, Y. Zou, H. Liang, T. He, X. Xu, Y. Zhang, Z. Ma, J. Wang, M. Zhang, Q. Li, C. Li, G. Long, X. Wan, Z. Yao and Y. Chen, *Sci. China Chem.*, 2022, **65**, 1362-1373.
2. H. Lai, H. Chen, Y. Zhu, H. Wang, Y. Li and F. He, *Macromolecules*, 2022, **55**, 3353-3360.
3. M. Li, H. Liang, C. Jiang, F. Huang, J. Wang, Y. Yang, X. Wan, C. Li, Z. Yao and Y. Chen, *Org. Electron.*, 2022, **106**, 106541.
4. L. Meng, M. Li, G. Lu, Z. Shen, S. Wu, H. Liang, Z. Li, G. Lu, Z. Yao, C. Li, X. Wan and Y. Chen, *Small*, 2022, **18**, 2201400.
5. J. Yuan, Y. Zhang, L. Zhou, G. Zhang, H.-L. Yip, T.-K. Lau, X. Lu, C. Zhu, H. Peng, P. A. Johnson, M. Leclerc, Y. Cao, J. Ulanski, Y. Li and Y. Zou, *Joule*, 2019, **3**, 1140-1151.
6. T. Duan, W. Feng, Y. Li, Z. Li, Z. Zhang, H. Liang, H. Chen, C. Zhong, S. Jeong, C. Yang, S. Chen, S. Lu, O. A. Rakitin, C. Li, X. Wan, B. Kan and Y. Chen, *Angew. Chem. Int. Ed.*, 2023, **62**, e202308832.
7. C. Zhang, M. Zhang, Q. Zhou, S. Chen, S. Kim, J. Yao, Z. Zhang, Y. Bai, Q. Chen, B. Chang, H. Fu, L. Xue, H. Wang, C. Yang and Z. G. Zhang, *Adv. Funct. Mater.*, 2023, **33**, 2214392.
8. W. Liu, J. Zhang, S. Xu and X. Zhu, *Sci. Bull.*, 2019, **64**, 1144-1147.
9. Z. Zhou, W. Liu, G. Zhou, M. Zhang, D. Qian, J. Zhang, S. Chen, S. Xu, C. Yang, F. Gao, H. Zhu, F. Liu and X. Zhu, *Adv. Mater.*, 2019, **32**, 1906324.
10. C. Zhu, J. Yuan, F. Cai, L. Meng, H. Zhang, H. Chen, J. Li, B. Qiu, H. Peng, S. Chen, Y. Hu, C. Yang, F. Gao, Y. Zou and Y. Li, *Energy Environ. Sci.*, 2020, **13**, 2459-2466.
11. H. Yu, Z. Qi, J. Zhang, Z. Wang, R. Sun, Y. Chang, H. Sun, W. Zhou, J. Min, H. Ade and H. Yan, *J. Mater. Chem. A*, 2020, **8**, 23756-23765.

12. H. Liang, X. Bi, H. Chen, T. He, Y. Lin, Y. Zhang, K. Ma, W. Feng, Z. Ma, G. Long, C. Li, B. Kan, H. Zhang, O. A. Rakitin, X. Wan, Z. Yao and Y. Chen, *Nat. Commun.*, 2023, **14**, 4707.

13. Y. Ding, S. Xiong, M. Li, M. Pu, Y. Zhu, X. Lai, Y. Wang, D. Qiu, H. Lai and F. He, *Small*, 2023, 2309169.

14. J. Wang, H. Chen, X. Xu, Z. Ma, Z. Zhang, C. Li, Y. Yang, J. Wang, Y. Zhao, M. Zhang, X. Wan, Y. Lu and Y. Chen, *J. Mater. Chem. A*, 2022, **10**, 16714-16721.

15. H. Chen, X. Cao, P. Wang, F. Huang, Y. Zhang, H. Liang, X. Bi, T. He, W. Feng, Y. Guo, Z. Ma, G. Long, Z. Yao, B. Kan, C. Li, X. Wan and Y. Chen, *J. Mater. Chem. A*, 2023, **11**, 25368-25376.

16. Y. Shi, Y. Chang, K. Lu, Z. Chen, J. Zhang, Y. Yan, D. Qiu, Y. Liu, M. A. Adil, W. Ma, X. Hao, L. Zhu and Z. Wei, *Nat. Commun.*, 2022, **13**, 3256.

17. Y.-J. Xue, Z.-Y. Lai, H.-C. Lu, J.-C. Hong, C.-L. Tsai, C.-L. Huang, K.-H. Huang, C.-F. Lu, Y.-Y. Lai, C.-S. Hsu, J.-M. Lin, J.-W. Chang, S.-Y. Chien, G.-H. Lee, U. S. Jeng and Y.-J. Cheng, *J. Am. Chem. Soc.*, 2023, **146**, 833-848.

18. L. Chen, C. Zhao, H. Yu, A. Sergeev, L. Zhu, K. Ding, Y. Fu, H. M. Ng, C. H. Kwok, X. Zou, J. Yi, X. Lu, K. S. Wong, H. Ade, G. Zhang and H. Yan, *Adv. Energy Mater.*, 2024, 2400285.

19. L. Zhou, H. Yu, J. Zhang, D. Qiu, Y. Fu, J. Yi, L. Xie, X. Li, L. Meng, J. Zhang, X. Lu, Z. Wei, Y. Li and H. Yan, *Angew. Chem. Int. Ed.*, 2024, **63**, e202319635.